



1 **Stationary Solutions and Oscillatory Dynamics in a**
2 **Mathematical Model of a Saturated Moist Atmosphere**

3 **Dalila Remaoun Bourega**

<https://orcid.org/0000-0002-0123-8446>

Laboratory of Research In Pure And Applied Mathematics (LRPAM),

Department of Mathematics, USTO-MB, 31000 Oran, Algeria

e-mail: dalila.bourega@univ-usto.dz

4 **Abstract**— This paper investigates the mathematical properties of a simplified atmospheric
5 system describing vertical air flows with water condensation. We focus on two primary aspects:
6 the long-term equilibrium and the transient oscillatory behavior. First, we provide a rigorous
7 proof for the existence and uniqueness of the stationary solution under specific technical condi-
8 tions, establishing a solid theoretical foundation for the model's stability. Secondly, we analyze
9 the oscillatory dynamics of the evolutionary system through numerical simulations. Our results
10 reveal damped oscillations in the air flow intensity $\alpha(t)$ and liquid water content $\Sigma(t)$, which are
11 interpreted as a self-regulating physical cycle driven by latent heat and droplet accumulation. By
12 establishing a qualitative analogy with a Volterra integro-differential equation, we demonstrate
13 that these oscillations are governed by memory effects, particularly the mean droplet residence
14 time b . The convergence of the evolutionary variables toward the calculated stationary values
15 provides a robust validation of the model's consistency. These findings contribute to a deeper
16 understanding of the physical mechanisms underlying storm formation and atmospheric stability.

17 **Keywords:** Atmospheric convection, Stationary solution, Volterra equation, Damped
18 oscillations, Existence and uniqueness.

19 **MSC (2020):** 86A10, 35Q35, 35F50

20 **1 INTRODUCTION**

21 Atmospheric phenomena such as cumulonimbus clouds, tropical cyclones (Montgomery
22 and Smith, 2017), and thunderstorms (Cotton et al., 2011) are primarily caused by upward
23 air flow and water vapor condensation. Accurately understanding and modeling these
24 complex processes is crucial for weather forecasting and climate studies. In previous
25 works (Aouaouda et al., 2019; Bourega et al., 2018; Ghomrani et al., 2015; Yashima, 2019),
26 researchers have examined systems of differential equations to describe these phenomena.
27 These systems typically involve unknown functions representing temperature (T), density
28 (ρ), vertical velocity (v_3), and the total amount of liquid water in the air (Σ).



29 A limitation observed in some older models, particularly those assuming a constant
30 cylindrical cross-section for air flow, was an unrealistic prediction of vertical velocity
31 increasing with altitude (Ghomrani et al., 2015). This behavior is not consistent with
32 natural observations. To address this, an improved model was introduced in (Bourega
33 et al., 2018), which considers air flow in a cylinder with a larger cross-section at higher
34 altitudes, effectively being “more open upwards.” In this corrected model, the vertical
35 flow velocity varies with time but does not change significantly with altitude.

36 Numerical calculations of this improved evolutionary model in (Bourega et al., 2018)
37 revealed an unexpected and significant finding: oscillations in the vertical flow velocity, ac-
38 companied by corresponding oscillations in the amount of liquid or solid water contained
39 in the air. Although oscillations of torrential rains have been previously addressed by
40 physicists, often in relation to gravitational waves (Plougonven and Zhang, 2014; Richiar-
41 done and Manfrin, 2003), our calculation results suggest an alternative mechanism. We
42 propose that the oscillation of rain during a thunderstorm may be caused by the cyclic
43 process of ascending moist air. This process leads to water vapor condensation, releasing
44 latent heat that warms the air and accelerates its ascent. Subsequently, the accumulation
45 of droplets produced by this process slows down the vertical air flow due to their weight.
46 This deceleration of air ascent reduces droplet production. The gradual disappearance
47 of droplets as they fall then allows the ascending flow of moist air to resume, creating a
48 self-sustaining oscillatory cycle.

49 We believe that such a calculation result, suggesting a new mechanism for rain oscil-
50 lation, warrants further investigation. This prompted us to focus on the stationary state,
51 or more precisely, the stationary solution, of this system. Understanding the existence
52 and uniqueness of stationary solutions is fundamental, especially when the evolutionary
53 system exhibits complex behaviors such as damped oscillations, as observed in (Bourega
54 et al., 2018). Recent advances in the qualitative behavior of such atmospheric mod-
55 els have highlighted the importance of establishing rigorous stationary states (Kouadri,
56 2022). The mathematical well-posedness of moisture dynamics with phase changes in
57 atmospheric systems has also been rigorously studied (Hittmeir et al., 2017), further mo-
58 tivating the analysis of stationary solutions in the present work. The stationary state
59 represents the physical equilibrium toward which the system tends to gravitate over the
60 long term.

61 The main objective of this article is to prove the existence and uniqueness of the
62 stationary solution for a simplified version of this system of equations. In this framework,
63 the vertical velocity v_3 is characterized by a parameter α , independent of altitude z .
64 Technically, our approach is inspired by the comparison theorem for ordinary differential
65 equations. This type of stability analysis for non-linear dynamical systems is essential in
66 fluid flow applications to ensure the physical consistency of the model (Mansour, 2021).
67 However, its direct application to a system of equations is not straightforward and requires
68 specific elaborations, which constitute the core of our mathematical contribution.

69 Beyond this theoretical result, we present numerical examples to illustrate the validity
70 of our proofs. Furthermore, we provide an in-depth analysis of the oscillatory dynamics
71 by drawing a qualitative analogy with the Volterra integro-differential equation. By intro-
72 ducing the concept of a memory effect— modeled by the mean droplet residence time — we



73 offer a deeper mathematical understanding of the mechanisms governing these oscillations
 74 and their convergence toward the stationary state.

75 2 THE FULL EVOLUTIONARY MODEL

In our previous article (Bourega et al., 2018), to describe the upward flow of air accompa-
 nied by water vapor condensation in the atmosphere, we proposed a system of equations
 for density (ρ), temperature (T), intensity coefficient (α), and normalized velocity (w).
 This model was developed by adopting the approximation $v(t, z) = \alpha(t)w(t, z)$, where v
 denotes the vertical component of the velocity. We assume quasi-stationary conditions
 for the spatial structure, neglecting the time derivatives of w , ρ , and T :

$$\partial_t w(t, z) \approx 0, \quad \partial_t \rho(t, z) \approx 0, \quad \partial_t T(t, z) \approx 0.$$

76 The system, defined in a cylindrical domain $\Omega_3 = \{(x, y, z) \in \mathbb{R}^3 \mid 0 \leq z \leq \bar{z}_1, (x^2 + y^2)\pi \leq$
 77 $S(z)\}$, is based on the fundamental equations of fluid mechanics (Landau and Lifshitz,
 78 1989). The main physical quantities are the vertical velocity v , temperature T , and
 79 density ρ . Pressure P is given by the ideal gas law:

$$P = R_1 \rho T, \quad R_1 = \frac{R_0}{\mu_a}, \quad (1)$$

80 where R_0 is the universal gas constant and μ_a is the molar mass of air.

81 Before presenting the complete system, we recall the quantities involved in the process
 82 of condensation or inverse sublimation of water vapor in the atmosphere. For simplicity,
 83 we approximate the latent heat of transition from water vapor to solid state by that from
 84 vapor to liquid state. Thus, L_{tr} denotes the latent heat of phase transition of water from
 85 gaseous to liquid or solid state. The density of saturated water vapor is denoted $\bar{\pi}_{vs}(T)$.
 86 Its dependence on temperature plays a crucial role. According to (Matveev, 2000), its
 87 expression is:

$$\bar{\pi}_{vs}(T) = \frac{E_0}{R_1 T} \cdot 10^{\frac{7.63(T-273.15)}{T-31.25}}, \quad E_0 = 6.107 \text{ mbar}. \quad (2)$$

88 For physical details on condensation or inverse sublimation (hereinafter simply referred
 89 to as *condensation*), see (Matveev, 2000; Prodi and Battaglia, 2004; Kikoine and Kikoine,
 90 1979).

91 The amount of condensation, H_{tr} , in air containing saturated water vapor and rising
 92 with a vertical velocity $v > 0$, is given by:

$$H_{tr} = \left(\bar{\pi}_{vs}(T) \frac{d}{dz} \log \rho - \frac{d}{dz} \bar{\pi}_{vs}(T) \right) v. \quad (3)$$

93 Derivation of the Turbulent Condensation Rate H_{tr}

To maintain saturation, the saturated mass concentration $q_s = \bar{\pi}_{vs}(T)/\rho$ must vary
 along the vertical motion v . The condensation rate H_{tr} is defined by the product of the



mass flow rate ρv and the spatial derivative of q_s : $H_{tr} = -v\rho \frac{d}{dz} \left(\frac{\bar{\pi}_{vs}}{\rho} \right)$. Applying the quotient rule for the derivative and factoring out ρ :

$$\frac{d}{dz} \left(\frac{\bar{\pi}_{vs}}{\rho} \right) = \frac{1}{\rho} \left(\frac{d\bar{\pi}_{vs}}{dz} - \bar{\pi}_{vs} \frac{1}{\rho} \frac{d\rho}{dz} \right).$$

94 Substituting this result into the expression for H_{tr} and using the identity $\frac{1}{\rho} \frac{d\rho}{dz} = \frac{d}{dz} \log \rho$,
95 we obtain:

$$H_{tr} = -v\rho \cdot \frac{1}{\rho} \left(\frac{d\bar{\pi}_{vs}}{dz} - \bar{\pi}_{vs} \frac{d}{dz} \log \rho \right)$$

$$H_{tr} = v \left(\bar{\pi}_{vs}(T) \frac{d}{dz} \log \rho - \frac{d}{dz} \bar{\pi}_{vs}(T) \right).$$

By decomposing ρ into $\rho = \rho_a + \rho_h$ (dry air density ρ_a , water vapor density ρ_h), and considering that phase transition only affects water vapor, we have:

$$\partial_t \rho + \nabla \cdot (\rho \mathbf{v}) = -H_{tr}.$$

96 The heat released by condensation is $L_{tr}H_{tr}$. Let Σ be the total amount of liquid or solid
97 water in the air. Neglecting viscosity and thermal conductivity, the air movement in the
98 “chimney” is described by:

$$S(z) \frac{\partial \rho}{\partial t} + \frac{\partial}{\partial z} (S(z) \rho v) = -S(z) H_{tr}, \quad (4)$$

$$\rho \left(\frac{\partial v}{\partial t} + v \frac{\partial v}{\partial z} \right) = -R_1 \frac{\partial}{\partial z} (\rho T) - g[\Sigma + \rho], \quad (5)$$

$$\rho c_v \left(\frac{\partial T}{\partial t} + v \frac{\partial T}{\partial z} \right) - R_1 T \left(\frac{\partial \rho}{\partial t} + v \frac{\partial \rho}{\partial z} \right) = (R_1 T + L_{tr}) H_{tr}, \quad (6)$$

99 where g is the acceleration due to gravity and c_v is the specific heat. For Σ in (5), we
100 define:

$$\Sigma(t) = \frac{1}{\bar{z}_1} \int_0^t \varphi(t-s) \int_0^{\bar{z}_1} \left(\bar{\pi}_{vs}(T(s, z)) \frac{\partial}{\partial z} \log \rho(s, z) - \frac{\partial}{\partial z} \bar{\pi}_{vs}(T(s, z)) \right) v(s, z) dz ds, \quad (7)$$

101 where $\varphi(\tau)$ represents the probability that a droplet remains in the air after time τ from
102 its creation (Ghomrani et al., 2015).

103 For this model to represent air movement in a thunderstorm, internal and external
104 pressures must be equal at the boundaries. We use a hydrostatic state system as a
105 reference for the external environment:

$$\rho c_v \frac{dT}{dz} - R_1 T \frac{d\rho}{dz} = \vartheta (R_1 T + L_{tr}) \left(\bar{\pi}_{vs}(T) \frac{d}{dz} \log \rho - \frac{d}{dz} \bar{\pi}_{vs}(T) \right), \quad (8)$$

$$R_1 \frac{d}{dz} (\rho T) = -g\rho. \quad (9)$$



106 Following (Ghomrani et al., 2015), we introduce the approximation $v(t, z) = \alpha(t)w(t, z)$.
 107 Substituting (3) into (4)–(6) yields:

$$S(z) \frac{\partial \rho}{\partial t} + \frac{\partial}{\partial z}(S(z)\rho w) = -S(z) \left(\bar{\pi}_{vs}(T) \frac{d}{dz} \log \rho - \frac{d}{dz} \bar{\pi}_{vs}(T) \right) w, \quad (10)$$

$$\rho c_v \frac{dT}{dz} - R_1 T \frac{d\rho}{dz} = (R_1 T + L_{tr}) \left(\bar{\pi}_{vs}(T) \frac{1}{\rho} \frac{d\rho}{dz} - \frac{d\bar{\pi}_{vs}(T)}{dT} \frac{dT}{dz} \right), \quad (11)$$

$$\rho w D + \alpha(t)^2 \rho w \frac{dw}{dz} + R_1 \rho \frac{dT}{dz} + R_1 T \frac{d\rho}{dz} = -g[\Sigma(t) + \rho], \quad (12)$$

$$\Sigma(t) = \frac{1}{\bar{z}_1} \int_0^t \varphi(t-s) \alpha(s) \int_0^{\bar{z}_1} \left(\bar{\pi}_{vs}(T) \frac{d}{dz} \log \rho - \frac{d}{dz} \bar{\pi}_{vs}(T) \right) w dz ds, \quad (13)$$

$$\frac{d}{dt} \alpha(t) = D(t). \quad (14)$$

108 The auxiliary unknown $D(t)$ allows the system to be treated as a control problem. The
 109 memory kernel φ is given by:

$$\varphi(\tau) = \exp\left(-\frac{\pi \tau^2}{4b^2}\right), \quad (15)$$

110 where the parameter b represents the mean droplet residence time.

111 3 THE STATIONARY SYSTEM AND ITS SIMPLIFICATION

112 This article focuses on the stationary solution of the system. The stationary solution
 113 must satisfy the system derived from (10)–(14) by setting $\frac{d}{dt} \alpha(t) = 0$ (hence $D(t) = 0$)
 114 and assuming $\alpha(t) = \alpha$ (a constant intensity coefficient) and $\Sigma(t) = \Sigma$ (a constant amount
 115 of total liquid water). Equations (12) and (13) are then replaced by:

$$\alpha^2 \rho w \frac{dw}{dz} + R_1 \rho \frac{dT}{dz} + R_1 T \frac{d\rho}{dz} = -g[\Sigma + \rho], \quad (16)$$

$$\Sigma = \alpha \frac{b}{\bar{z}_1} \int_0^{\bar{z}_1} \left(\bar{\pi}_{vs}(T) \frac{d}{dz} \log \rho - \frac{d}{dz} \bar{\pi}_{vs}(T) \right) w dz, \quad (17)$$

116 where $b = \int_0^\infty \varphi(\tau) d\tau$. It should be noted that Σ represents a density, so its unit is in
 117 g/m^3 .

118 In (Ghomrani et al., 2015), the assumption of a constant cylindrical cross-section $S(z)$
 119 led to an unrealistic increase in velocity with altitude. To correct this, (Bourega et al.,
 120 2018) proposed choosing $S(z)$ such that the normalized velocity w remains close to 1.
 121 Following this idea, if we assume that $S(z)$ is not a priori given but is determined a
 122 posteriori by the solution (ρ, T) and by setting $w \equiv 1$, we can find ρ, T, α satisfying the
 123 simplified system.



124 We now derive the explicit expression for $S(z)$ by imposing the condition of a uniform
 125 normalized velocity, $w(t, z) \equiv 1$. Substituting $w = 1$ into the quasi-stationary continuity
 126 equation (10) yields:

$$S(z) \frac{\partial \rho}{\partial t} + \frac{\partial}{\partial z} (S(z) \rho) = -S(z) H_{tr}^{\text{cond}}, \quad (18)$$

where $H_{tr}^{\text{cond}} = (\bar{\pi}_{vs}(T) \frac{d}{dz} \log \rho - \frac{d}{dz} \bar{\pi}_{vs}(T))$ is the term in parenthesis in Equation (3). For the fully stationary case ($\partial_t \rho = 0$), the equation simplifies to the conservation law:

$$\frac{d}{dz} (S \rho) = -S \cdot H_{tr}^{\text{cond}}.$$

Expanding the derivative on the Left-Hand Side (LHS) and substituting the expression for H_{tr}^{cond} gives:

$$\rho \frac{dS}{dz} + S \frac{d\rho}{dz} = -S \left(\bar{\pi}_{vs}(T) \frac{d}{dz} \log \rho - \frac{d}{dz} \bar{\pi}_{vs}(T) \right).$$

127 Dividing by $S\rho$ and reorganizing the terms to separate the S dependence leads to:

$$\begin{aligned} \frac{1}{S} \frac{dS}{dz} &= -\frac{1}{\rho} \frac{d\rho}{dz} - \frac{1}{\rho} \left(\bar{\pi}_{vs}(T) \frac{d}{dz} \log \rho - \frac{d}{dz} \bar{\pi}_{vs}(T) \right) \\ \frac{d}{dz} \log S &= -\frac{d}{dz} \log \rho + \frac{1}{\rho} \left(\frac{d}{dz} \bar{\pi}_{vs}(T) - \bar{\pi}_{vs}(T) \frac{d}{dz} \log \rho \right) \end{aligned}$$

Using the identity $\frac{d}{dz} \left(\frac{\bar{\pi}_{vs}}{\rho} \right) = \frac{1}{\rho} \left(\frac{d\bar{\pi}_{vs}}{dz} - \bar{\pi}_{vs} \frac{d}{dz} \log \rho \right)$ (derived in Section 2, but without the ρ factor), the expression simplifies to the logarithmic derivative of the term $\frac{\bar{\pi}_{vs}}{\rho}$:

$$\frac{d}{dz} \log S = -\frac{d}{dz} \log \rho - \frac{d}{dz} \left(\frac{\bar{\pi}_{vs}(T)}{\rho} \right).$$

Integrating this equation from $z = 0$ to z :

$$\log \left(\frac{S(z)}{S(0)} \right) = -\log \left(\frac{\rho(z)}{\rho(0)} \right) - \left[\frac{\bar{\pi}_{vs}(T(z))}{\rho(z)} - \frac{\bar{\pi}_{vs}(T_0)}{\rho_0} \right].$$

128 Solving for $S(z)$ finally yields:

$$S(z) = \frac{\rho_0 S(0)}{\rho(z)} \exp \left(\frac{\bar{\pi}_{vs}(T(z))}{\rho(z)} - \frac{\bar{\pi}_{vs}(T_0)}{\rho_0} \right). \quad (19)$$

129 **Note on the Choice $w \equiv 1$:** The original full evolutionary system only determines
 130 the product $v(t, z) = \alpha(t)w(t, z)$, not the spatial structure $w(t, z)$ and the temporal
 131 intensity $\alpha(t)$ separately. The choice $\mathbf{w}(\mathbf{z}) \equiv \mathbf{1}$ in the stationary analysis is therefore
 132 a normalization made to disentangle the variables. By fixing $w(z) \equiv 1$, all variations
 133 in the flow velocity are carried by the temporal coefficient $\alpha(t)$ in the evolutionary
 134 model, and by the constant α in the stationary system. This normalization is just-
 135 ified because the volume $S(z)$ has been chosen precisely to make the normalized
 136 velocity w close to unity, thereby simplifying the study of the remaining equations.



137 Thus, we are interested in the following system of equations for the variables (ρ, T, α) on
 138 $0 < z < \bar{z}_1$:

$$\rho c_v \frac{dT}{dz} - R_1 T \frac{d\rho}{dz} = (R_1 T + L_{tr}) \left(\bar{\pi}_{vs}(T) \frac{1}{\rho} \frac{d\rho}{dz} - \frac{d\bar{\pi}_{vs}(T)}{dT} \frac{dT}{dz} \right), \quad (20)$$

$$R_1 \rho \frac{dT}{dz} + R_1 T \frac{d\rho}{dz} = -g[\Sigma + \rho], \quad (21)$$

$$\Sigma = \alpha \frac{b}{\bar{z}_1} \int_0^{\bar{z}_1} \left(\bar{\pi}_{vs}(T) \frac{d}{dz} \log \rho - \frac{d}{dz} \bar{\pi}_{vs}(T) \right) dz, \quad (22)$$

139 This system is considered with the conditions:

$$\rho(0) = \rho_0, \quad T(0) = T_0, \quad (23)$$

$$\rho(\bar{z}_1) T(\bar{z}_1) = q_0. \quad (24)$$

140 The study of stationary solutions is a common approach in many fields of physics and
 141 engineering to analyze the long-term behavior of systems, as exemplified by works on
 142 glacier dynamics (Bogovskii et al., 2010).

143 4 PRELIMINARIES FOR THE STATIONARY SOLUTION

144 In the phenomenon of water vapor condensation caused by upward air flow, the saturated
 145 vapor density function $\bar{\pi}_{vs}(T)$ plays a crucial role. Its properties influence the solution of
 146 the system of equations (20)–(22). We define the expression for $\bar{\pi}_{vs}(T)$ by:

$$\bar{\pi}_{vs}(T) = \frac{E_0}{R_1 T} \cdot 10^{\frac{7.63(T-273.15)}{T-31.25}}, \quad E_0 = 6.107 \text{ (mbar)}. \quad (25)$$

147 which is given by physics (see for example (Matveev, 2000)). We consider this expression
 148 only for $T > 31.25$ (K). If, in the problem, we neglect condition (24) and set $\alpha = 0$ (and
 149 thus $\Sigma = 0$), then ρ and T can be determined by equations (20), (21) and condition (23).

150 Consider a parameter $\vartheta \in [0, 1]$ introduced on the right-hand side of equation (20).
 151 We define the problem of the hydrostatic state of partially moist air as follows:

$$\rho c_v \frac{dT}{dz} - R_1 T \frac{d\rho}{dz} = \vartheta (R_1 T + L_{tr}) \left(\bar{\pi}_{vs}(T) \frac{d}{dz} \log \rho - \frac{d}{dz} \bar{\pi}_{vs}(T) \right), \quad (26)$$

$$R_1 \frac{d}{dz}(\rho T) = -g\rho, \quad (27)$$

$$\rho(0) = \rho_0, \quad T(0) = T_0. \quad (28)$$

152 We denote by $(\rho_{hs}^{[0]}, T_{hs}^{[0]})$ the solution of problem (26)–(28) with $\vartheta \equiv 0$, and by $(\rho_{hs}^{[1]}, T_{hs}^{[1]})$
 153 that of the case $\vartheta \equiv 1$. Before stating Lemma 1, we define $\Theta_- = 31.25$ (K),

$$\Theta_+ = 31.25 + \frac{1}{7} \log_{10}(1845.697) + \sqrt{\left(31.25 + \frac{1}{7} \log_{10}(1845.697) \right)^2 - 976.5625} \approx 1275.9 \text{ (K)}, \quad (29)$$



154 and

$$\bar{z}^* = \frac{c_v + R_1}{g}(T_0 - 31.25). \quad (30)$$

155 The condition $\Theta_- < T < \Theta_+$ guarantees the inequality $T \frac{d}{dT} \log(\bar{\pi}_{vs}(T)) > \frac{c_v}{R_1} = \frac{5}{2}$, which
 156 is necessary in the proof. Note that $T_{hs}^{[0]}(\bar{z}^*) = 31.25$.

157 **Physical vs. Analytical Significance of the Thresholds** The defined thresh-
 158 olds $\Theta_- = 31.25$ K, $\Theta_1 \approx 66$ K, and $\Theta_+ \approx 1275.9$ K are purely analytical bounds
 159 derived from the structure of $\bar{\pi}_{vs}(T)$ ((25)). The lower bound Θ_- corresponds to the
 160 temperature where the denominator of the vapor density expression becomes zero. The
 161 bounds Θ_1 and Θ_+ are the analytical limits introduced to guarantee the crucial inequality
 162 $T \frac{d}{dT} \log(\bar{\pi}_{vs}(T)) > c_v/R_1$ used in the monotonicity lemmata. Since the temperatures of
 163 the physical phenomena of interest satisfy $100 \text{ K} < T < 373.15 \text{ K}$, all analytical condi-
 164 tions ($\Theta_- < T < \Theta_+$) are automatically satisfied. Therefore, these bounds impose no
 165 practical restriction on the physical domain of the solution, serving only as a technical
 166 requirement for the mathematical proof structure. We now state the following lemma:

167 **Lemma 1.** *We assume that $\rho_0 > 0$ and $\Theta_- < T_0 < \Theta_+$. Then the system of equations*
 168 *(26)–(27) with condition (28) admits a unique continuously differentiable solution (ρ, T)*
 169 *on the interval $[0, \bar{z}^*$. Furthermore, the functions $\rho(z)$ and $T(z)$ are strictly decreasing,*
 170 *and we have*

$$T(z) \geq T_{hs}^{[0]}(z) \quad \forall z \in [0, \bar{z}^*]. \quad (31)$$

171 **Proof .** It is clear that the system of equations (26)–(27) with initial data $\rho_0 > 0$
 172 and $\Theta_- < T_0 < \Theta_+$ admits a unique C^1 solution in a sufficiently small interval. To
 173 prove the existence and uniqueness of the solution in $[0, \bar{z}^*$, it suffices to demonstrate
 174 that if the solution exists in an interval $[0, \bar{z}]$ with $0 < \bar{z} < \bar{z}^*$, then $0 < \inf_{0 \leq z < \bar{z}} \rho(z) \leq$
 175 $\sup_{0 \leq z < \bar{z}} \rho(z) < \infty$ and $\Theta_- < \inf_{0 \leq z < \bar{z}} T(z) \leq \sup_{0 \leq z < \bar{z}} T(z) < \Theta_+$. For this, we use the
 176 properties illustrated in the following lemmas.

177 **Lemma 2.** *Assume that $\rho_0 > 0$ and $\Theta_- < T_0 < \Theta_+$ and that (ρ, T) , with $\rho > 0$ and*
 178 *$\Theta_- < T < \Theta_+$, is the solution of the system of equations (26)–(27) with condition (28)*
 179 *in an interval $[0, \bar{z}]$, $0 < \bar{z} \leq \bar{z}^*$. Then the functions $\rho(z)$ and $T(z)$ are strictly decreasing*
 180 *in the interval $[0, \bar{z}]$ and we have*

$$\frac{d}{dz} \left(\frac{\bar{\pi}_{vs}(T(z))}{\rho(z)} \right) \leq 0 \quad \forall z \in [0, \bar{z}]. \quad (32)$$

181 **Proof.** It is convenient to transform equation (26) into the form:

$$\frac{d}{dz} \log \left(\frac{T^{c_v}}{\rho^{R_1}} \right) = -\vartheta \left(R_1 + \frac{L_{tr}}{T} \right) \frac{d}{dz} \left(\frac{\bar{\pi}_{vs}(T)}{\rho} \right). \quad (33)$$

182 Equation (33) is obtained by dividing Equation (26) by ρT and utilizing two key identities:



183 1. The logarithmic derivative of the left-hand side (LHS):

$$\frac{d}{dz}(c_v \log T - R_1 \log \rho) = \frac{d}{dz} \log \left(\frac{T^{c_v}}{\rho^{R_1}} \right)$$

184 2. The compact form of the right-hand side (RHS) using $q_s = \bar{\pi}_{vs}/\rho$:

$$\frac{1}{\rho} \left(\bar{\pi}_{vs} \frac{d}{dz} \log \rho - \frac{d}{dz} \bar{\pi}_{vs} \right) = -\frac{d}{dz} \left(\frac{\bar{\pi}_{vs}}{\rho} \right)$$

185 Combining these steps yields Equation (33).

186 Furthermore, from equation (27), it immediately follows that:

$$\frac{d}{dz}(\rho(z)T(z)) = -\frac{g}{R_1}\rho(z) < 0 \quad \forall z \in [0, \bar{z}].$$

187 Therefore, it is impossible that $\frac{d}{dz}\rho(z) \geq 0$ and $\frac{d}{dz}T(z) \geq 0$ simultaneously.

188 Now we show that ρ and T are both strictly decreasing. Suppose by contradiction that
 189 $\frac{d}{dz}T(z_0) \geq 0$ at some z_0 . Then from $\frac{d}{dz}(\rho T) < 0$, we must have $\frac{d}{dz}\rho(z_0) < 0$. But then
 190 the LHS of (33) would be strictly positive, while the RHS would be non-positive, which
 191 is impossible. Similarly, if $\frac{d}{dz}\rho(z_0) \geq 0$, then $\frac{d}{dz}T(z_0) < 0$, making the LHS negative while
 192 the RHS non-negative. Thus, we must have $\frac{d}{dz}\rho(z) < 0$ and $\frac{d}{dz}T(z) < 0$ for all $z \in [0, \bar{z}]$.

193 To prove (32), we assume by contradiction that there exists a $z_0 \in [0, \bar{z}]$ such that:

$$\frac{d}{dz} \left(\frac{\bar{\pi}_{vs}(T(z_0))}{\rho(z_0)} \right) > 0.$$

194 This implies that at z_0 :

$$\frac{1}{\rho} \frac{d\bar{\pi}_{vs}}{dT} \frac{dT}{dz} - \frac{\bar{\pi}_{vs}}{\rho^2} \frac{d\rho}{dz} > 0 \quad \iff \quad -\frac{d\rho}{dz} > -\frac{\rho}{\bar{\pi}_{vs}(T)} \frac{d\bar{\pi}_{vs}(T)}{dT} \frac{dT}{dz}.$$

195 Substituting this into the LHS of (26) at z_0 gives:

$$\text{LHS} > \rho \left(c_v - R_1 T \frac{d}{dT} \log(\bar{\pi}_{vs}(T)) \right) \frac{dT}{dz}.$$

196 Under the condition $\Theta_- < T < \Theta_+$, the term in parenthesis is negative. Since $\frac{dT}{dz} < 0$,
 197 the product is strictly positive (LHS > 0).

198 Meanwhile, the right-hand side of (26) at z_0 is:

$$\text{RHS} = \vartheta(R_1 T + L_{tr}) \rho \left[-\frac{d}{dz} \left(\frac{\bar{\pi}_{vs}}{\rho} \right) \right] < 0.$$

199 The contradiction (LHS > 0 and RHS < 0) proves that $\frac{d}{dz}(\bar{\pi}_{vs}/\rho) \leq 0$. The lemma is
 200 proven. \square



201 **Lemma 3.** Assume that $\rho_0 > 0$ and $\Theta_- < T_0 < \Theta_+$ and that (ρ, T) , with $\rho > 0$ and
 202 $\Theta_- < T < \Theta_+$, is the solution of the system of equations (26)–(27) with condition (28)
 203 in an interval $[0, \bar{z}]$, $0 < \bar{z} \leq \bar{z}^*$. Then we have

$$T(z) \geq T_{hs}^{[0]}(z) \quad \forall z \in [0, \bar{z}]. \quad (34)$$

204 **Proof .** Define

$$\varphi_1(z) = \vartheta \int_0^z \left(R_1 + \frac{L_{tr}}{T(z')} \right) \left(-\frac{d}{dz'} \left(\frac{\bar{\pi}_{vs}(T(z'))}{\rho(z')} \right) \right) dz'. \quad (35)$$

205 By virtue of Lemma 2, we have

$$\varphi_1(z) \geq 0 \quad \forall z \in [0, \bar{z}]. \quad (36)$$

Furthermore, from equation (26) (or (33)), we deduce

$$\frac{T^{c_v}}{\rho^{R_1}} = \frac{T_0^{c_v}}{\rho_0^{R_1}} e^{\varphi_1},$$

206 OR

$$\rho = \rho_0 \frac{T^{c_v/R_1}}{T_0^{c_v/R_1}} e^{-\varphi_1/R_1}. \quad (37)$$

207 Substituting (37) into (27), we obtain

$$R_1 \frac{d}{dz} \left(T^{(c_v+R_1)/R_1} e^{-\varphi_1/R_1} \right) = -g T^{c_v/R_1} e^{-\varphi_1/R_1}. \quad (38)$$

Justification for the substitution $y(z)$: The variable $y(z)$ is chosen precisely because it is the exact expression inside the derivative on the Left-Hand Side (LHS) of (38). This enables the immediate transformation of the LHS into $R_1 dy/dz$. Simultaneously, the RHS simplifies because $T^{c_v/R_1} e^{-\varphi_1/R_1}$ can be fully expressed as a power of $y(z)$, leading to the compact form (39) in the next step. Indeed, if we set $y = T^{(c_v+R_1)/R_1} e^{-\varphi_1/R_1}$, equation (38) transforms into

$$R_1 \frac{d}{dz} y = -g y^{c_v/(c_v+R_1)} e^{-\varphi_1/(c_v+R_1)},$$

208 OR

$$(c_v + R_1) \frac{d}{dz} y^{R_1/(c_v+R_1)} = -g e^{-\varphi_1/(c_v+R_1)}. \quad (39)$$

The solution of equation (39) with initial condition $(y(0))^{R_1/(c_v+R_1)} = T_0$ is

$$y^{R_1/(c_v+R_1)} = T_0 - \frac{g}{(c_v + R_1)} \int_0^z e^{-\varphi_1/(c_v+R_1)} dz'.$$

209 Therefore, $T(z)$ has the form

$$T(z) = \left(T_0 - \frac{g}{(c_v + R_1)} \int_0^z e^{-\varphi_1/(c_v+R_1)} dz' \right) e^{\varphi_1/(c_v+R_1)}. \quad (40)$$



If $\varphi_1 \geq 0$, then we have $e^{-\varphi_1/(c_v+R_1)} \leq 1 \leq e^{\varphi_1/(c_v+R_1)}$. Therefore, by virtue of (36), we have

$$T(z) \geq T_0 - \frac{g}{(c_v + R_1)} z = T_{hs}^{[0]}(z).$$

210 The lemma is proven. □

211 **Continuation of the proof of Lemma 1** Since $T(z)$ is decreasing according to Lemma
212 2, and considering (34), we have

$$0 < \Theta_- < T_{hs}^{[0]}(z) \leq T(z) \leq T_0 < \Theta_+ \quad \forall z \in [0, \bar{z}]. \quad (41)$$

213 Furthermore, since for all $T > \Theta_-$ and for all $\rho > 0$, we have $\frac{\bar{\pi}_{vs}(T)}{\rho} > 0$, from Lemmas 2
214 and 3, we deduce that

$$0 \leq \varphi_1(z) \leq \left(R_1 + \frac{L_{tr}}{T_{hs}^{[0]}(z)} \right) \frac{\bar{\pi}_{vs}(T_0)}{\rho_0} \leq \left(R_1 + \frac{L_{tr}}{\Theta_-} \right) \frac{\bar{\pi}_{vs}(T_0)}{\rho_0} \equiv K_{\varphi_1} < \infty. \quad (42)$$

215 Consequently, from (37), (42), and Lemma 2, we obtain

$$0 < K_{\rho}^- \equiv \rho_0^{R_1} \frac{\Theta_-^{c_v/R_1}}{T_0^{c_v/R_1}} e^{-K_{\varphi_1}/R_1} \leq \rho_0^{R_1} \frac{(T_{hs}^{[0]}(z))^{c_v/R_1}}{T_0^{c_v/R_1}} e^{-K_{\varphi_1}/R_1} \leq \rho(z) \leq \rho_0 < \infty \quad (43)$$

216 for all $z \in [0, \bar{z}]$. Inequalities (41) and (43) allow us to extend the solution (ρ, T) with
217 its properties of strict decrease and inequality (34) over the entire interval $[0, \bar{z}^*]$. The
218 proposition is proven. □

219 5 EXISTENCE AND UNIQUENESS OF THE STATIONARY SOLUTION

220 We will prove the existence and uniqueness of the solution to problem (20)–(24), under a
221 technical condition:

$$T > \Theta_1, \quad (44)$$

222 where Θ_1 is defined by the following relations:

$$\frac{c_v + R_1}{R_1} \bar{\pi}_{vs}(T) - \frac{\bar{\pi}_{vs}(T)}{T} - \frac{d\bar{\pi}_{vs}(T)}{dT} > 0 \quad \text{if } T > \Theta_1, \quad (45)$$

$$\frac{c_v + R_1}{R_1} \bar{\pi}_{vs}(T) - \frac{\bar{\pi}_{vs}(T)}{T} - \frac{d\bar{\pi}_{vs}(T)}{dT} < 0 \quad \text{if } \Theta_- < T < \Theta_1; \quad (46)$$

223 we estimate the value of Θ_1 to be 66.09 (K). Condition (44) simplifies the proof of exist-
224 tence and uniqueness of the solution. It is possible to study the existence and uniqueness
225 of the solution in a more general case, but this would require much more complicated
226 arguments. Furthermore, the case $T \leq \Theta_1$ ($\Theta_1 \approx 66.09$ (K)) is infrequent (at least con-
227 cerning Earth’s atmosphere). For this reason, in the present article, we will show the
228 existence and uniqueness of the solution under condition (44).

229 Then for problem (20)–(24) we have the following result (in the statement, $\rho_{hs}^{[1]}$ and
230 $T_{hs}^{[1]}$ are the functions defined by problem (26)–(28) and condition (44)).



231 **Proposition 5.1.** Consider two real numbers $\rho_0 > 0$ and $T_0 \in]\Theta_1, \Theta_+[$. Let $\bar{z}_1 \in]0, \bar{z}^*[$
 232 (where \bar{z}^* is the number defined in (30)) under the condition $T_{hs}^{[1]}(\bar{z}_1) > \Theta_1$. Then there
 233 exists a number \bar{Q}_0 with $0 < \bar{Q}_0 < \rho_{hs}^{[1]}(\bar{z}_1)T_{hs}^{[1]}(\bar{z}_1)$, and for each $q_0 \in]\bar{Q}_0, \rho_{hs}^{[1]}(\bar{z}_1)T_{hs}^{[1]}(\bar{z}_1)[$
 234 there exists a unique solution (ρ, T, α) to problem (20)–(24) such that

$$\inf\{T(\bar{z}_1) \mid (\rho, T) = \text{Sol}(q_0)\} = \Theta_1, \quad (47)$$

235 where $\text{Sol}(q_0)$ is the solution of problem (20)–(24) with $q_0 \in]\bar{Q}_0, \rho_{hs}^{[1]}(\bar{z}_1)T_{hs}^{[1]}(\bar{z}_1)[$.

236 **Proof .** To prove the proposition, consider the auxiliary equation:

$$\frac{dP}{dz} = -g\rho - c_0 \quad (48)$$

237 with a constant $c_0 \geq 0$. We therefore have the following lemma:

238 **Lemma 4.** Consider the numbers ρ_0, T_0, \bar{z}_1 as in Proposition 5.1. If (ρ, T) is a solution
 239 in the interval $[0, \bar{z}_1]$ of problem (20), (48), (23) with some $c_0 \geq 0$, then $\rho(z)$ and $T(z)$
 240 are decreasing functions.

On the other hand, let $c^{(i)}$ and $c^{(ii)}$ be two numbers such that $0 \leq c^{(i)} < c^{(ii)}$. If
 $(\rho^{(i)}, T^{(i)})$ and $(\rho^{(ii)}, T^{(ii)})$ are the solutions in the interval $[0, \bar{z}_1]$ of problem (20), (48),
 (23) with $c_0 = c^{(i)}$ and $c_0 = c^{(ii)}$ respectively, solutions that satisfy the relations:

$$\rho^{(i)}(z) > 0, \quad \rho^{(ii)}(z) > 0, \quad \Theta_1 < T^{(i)}(z) < \Theta_+, \quad \Theta_1 < T^{(ii)}(z) < \Theta_+.$$

241 Then we have

$$T^{(ii)}(z) < T^{(i)}(z) \quad \forall z \in]0, \bar{z}_1], \quad (49)$$

$$\rho^{(ii)}(z)T^{(ii)}(z) < \rho^{(i)}(z)T^{(i)}(z) \quad \forall z \in]0, \bar{z}_1]. \quad (50)$$

242 The proof of Lemma 4 will be given in Section 6. In this section, we assume it to be
 243 true and continue the proof of Proposition 5.1.

244 **Continuation of the proof of Proposition 5.1** Let (ρ_{c_0}, T_{c_0}) be the solution (ρ, T)
 245 of problem (20), (48), (23) with c_0 . The strict monotonicity of the solution $\nu(c_0)$ is
 246 guaranteed by Lemma 4. Specifically, the ordering of the solutions ($T^{(ii)} < T^{(i)}$ for
 247 $c^{(ii)} > c^{(i)}$) is established by the sign of the derivative $\partial_\rho \mathbf{D}_1 > \mathbf{0}$ (proven in Section 6
 248 under the condition $T > \Theta_1$), which prevents the crossing of the temperature profiles $T^{(i)}$
 249 and $T^{(ii)}$.

250 By virtue of the strict inequalities (49), (50), and the continuous dependence of the
 251 solution on c_0 , we define the domain of c_0 as $[0, \bar{C}_0]$, where \bar{C}_0 is a finite value such that:

$$\lim_{c_0 \rightarrow \bar{C}_0^-} T_{c_0}(\bar{z}_1) = \Theta_1 \quad (51)$$

252 The finiteness of \bar{C}_0 is guaranteed by the lower bound of the temperature domain, $T > \Theta_1$.
 253 Since $T(z)$ must remain above Θ_1 for the solution to exist (otherwise the rate of decrease



254 would become singular), the rate of dissipation (proportional to c_0) cannot increase in-
 255 definitely.

The relation (51), the decrease of functions $\rho(z)$ and $T(z)$, and (49), guarantee that, for any $c_0 \in [0, \bar{C}_0[$, we have

$$0 < \rho_{c_0}(z) \leq \rho_0, \quad \Theta_1 < T_{c_0}(z) \leq T_0 < \Theta_+$$

256 for $z \leq \bar{z}_1$. This implies that for any $c_0 \in [0, \bar{C}_0[$ the solution (ρ_{c_0}, T_{c_0}) exists over the
 257 entire interval $[0, \bar{z}_1]$.

258 Now, we define the function $\nu(c_0)$ representing the value of the product ρT at the
 259 top boundary $z = \bar{z}_1$. This quantity is directly proportional to the pressure $P(\bar{z}_1) =$
 260 $R_1 \rho(\bar{z}_1) T(\bar{z}_1)$ at that height:

$$\nu(c_0) = \rho_{c_0}(\bar{z}_1) T_{c_0}(\bar{z}_1). \quad (52)$$

261 By virtue of the continuous dependence of the solution on the data, the function $\nu(c_0)$ is
 262 continuous in c_0 and, according to Lemma 4, it is strictly decreasing. Therefore, if q_0 is
 263 given in the admissible interval, then there exists a unique c_0 given by:

$$c_0 = \nu^{-1}(q_0). \quad (53)$$

264 With the determined value of c_0 , we can solve problem (20), (48), (23) and obtain the
 265 solution $(\rho, T) = (\rho_{c_0}, T_{c_0})$. We can then determine the value of the integral:

$$\int_0^{\bar{z}_1} \left(\bar{\pi}_{vs}(T) \frac{d}{dz} \log \rho - \frac{d}{dz} \bar{\pi}_{vs}(T) \right) dz. \quad (54)$$

266 By setting:

$$\alpha = \frac{c_0 \bar{z}_1}{gb} \left[\int_0^{\bar{z}_1} \left(\bar{\pi}_{vs}(T) \frac{d}{dz} \log \rho - \frac{d}{dz} \bar{\pi}_{vs}(T) \right) dz \right]^{-1}, \quad (55)$$

267 we will have constructed the solution (ρ, T, α) of problem (20)–(24). The uniqueness of
 268 the solution follows from the strict monotonicity of the function $\nu(c_0)$ and the uniqueness
 269 of the local solution of the system of equations (20), (48). Characterization (47) is also
 270 justified by Lemma 4. The Proposition 5.1 is proven. \square

271 6 PROOF OF LEMMA 4

272 **Lemma 5.** *If the functions $\rho(z)$ and $T(z)$ satisfy equations (20) and (48) in the neigh-*
 273 *borhood of z , then*

$$\frac{dT}{dz} = D_1(\rho, T, c_0), \quad \frac{d\rho}{dz} = D_2(\rho, T, c_0), \quad (56)$$

274

$$\frac{\partial D_1(\rho, T, c_0)}{\partial \rho} > 0 \quad \text{with } T > \Theta_1, \quad (57)$$

275 where

$$D_1(\rho, T, c_0) = - \frac{\left(\frac{R_1 T + L_{tr}}{R_1 \rho T} \bar{\pi}_{vs}(T) + 1 \right) (g\rho + c_0)}{\left[\rho(c_v + R_1) + (R_1 T + L_{tr}) \left(\frac{\bar{\pi}_{vs}(T)}{T} + \frac{d\bar{\pi}_{vs}(T)}{dT} \right) \right]}, \quad (58)$$



276

$$D_2(\rho, T, c_0) = - \frac{\left(\frac{R_1 T + L_{tr}}{R_1 \rho} \frac{d\bar{\pi}_{vs}(T)}{dT} + \frac{c_v}{R_1} \right) (g\rho + c_0)}{\left[T(c_v + R_1) + (R_1 T + L_{tr}) \left(\frac{\bar{\pi}_{vs}(T)}{\rho} + \frac{c_v}{R_1} \frac{d\bar{\pi}_{vs}(T)}{dT} \right) \right]}. \quad (59)$$

Proof. Since equations (20) and (48) are linear with respect to $\frac{dT}{dz}$ and $\frac{d\rho}{dz}$, by substituting

$$\frac{d\rho}{dz} = -\frac{\rho}{T} \frac{dT}{dz} - \frac{g\rho + c_0}{R_1 T}$$

and

$$\frac{dT}{dz} = -\frac{T}{\rho} \frac{d\rho}{dz} - \frac{g\rho + c_0}{R_1 \rho}$$

277 which are obtained from (48) into (20), we obtain (56) with (58) and (59).

278 We also have

$$\frac{\partial D_1(\rho, T, c_0)}{\partial \rho} = \frac{E(\rho, T, c_0)}{\left[\rho(c_v + R_1) + (R_1 T + L_{tr}) \left(\frac{\bar{\pi}_{vs}(T)}{T} + \frac{d\bar{\pi}_{vs}(T)}{dT} \right) \right]^2}, \quad (60)$$

279 where

$$\begin{aligned} E(\rho, T, c_0) &= \left(\frac{R_1 T + L_{tr}}{R_1 \rho T} \bar{\pi}_{vs}(T) + 1 \right) (g\rho + c_0)(c_v + R_1) \\ &\quad + \left[\rho(c_v + R_1) + (R_1 T + L_{tr}) \left(\frac{\bar{\pi}_{vs}(T)}{T} + \frac{d\bar{\pi}_{vs}(T)}{dT} \right) \right] \\ &\quad \times \left(\frac{R_1 T + L_{tr}}{R_1 \rho^2 T} \bar{\pi}_{vs}(T)(g\rho + c_0) - g \left(\frac{R_1 T + L_{tr}}{R_1 \rho T} \bar{\pi}_{vs}(T) + 1 \right) \right). \end{aligned}$$

Now, since

$$\frac{R_1 T + L_{tr}}{R_1 \rho^2 T} \bar{\pi}_{vs}(T)(g\rho + c_0) - g \left(\frac{R_1 T + L_{tr}}{R_1 \rho T} \bar{\pi}_{vs}(T) + 1 \right) \geq -g,$$

280 we have

$$\begin{aligned} E(\rho, T, c_0) &\geq \left(\frac{R_1 T + L_{tr}}{R_1 \rho T} \bar{\pi}_{vs}(T) + 1 \right) g\rho(c_v + R_1) - g \left[\rho(c_v + R_1) + (R_1 T + L_{tr}) \left(\frac{\bar{\pi}_{vs}(T)}{T} + \frac{d\bar{\pi}_{vs}(T)}{dT} \right) \right] \\ &= g(R_1 T + L_{tr}) \left[\frac{c_v + R_1}{R_1} \bar{\pi}_{vs}(T) - \frac{\bar{\pi}_{vs}(T)}{T} - \frac{d\bar{\pi}_{vs}(T)}{dT} \right], \end{aligned}$$

281 Therefore, considering condition (45), we obtain (57). □

282 **Note on the Latent Heat L_{tr} :** It is important to highlight that the factor $g(R_1 T +$
 283 $L_{tr})$ remains strictly positive. This holds true regardless of whether L_{tr} is treated
 284 as a constant (as simplified in some analytic proofs) or as a temperature-dependent
 285 function $L_{tr}(T)$ (as used in the numerical scheme), provided that T remains within
 286 its physical domain. Crucially, the dependence of L_{tr} on T does not alter the sign
 287 of the derivative $\partial_\rho D_1$ which is essential for establishing the monotonicity of the
 288 solution and thus the uniqueness (Lemma 4).



289 We recall the behavior of the solution in the neighborhood of $z = 0$.

290 **Lemma 6.** *If $0 \leq c^{(i)} < c^{(ii)}$, then there exists a number $\varepsilon_z > 0$ such that*

$$\rho^{(ii)}(z) < \rho^{(i)}(z), \quad T^{(ii)}(z) < T^{(i)}(z) \quad \forall z \in]0, \varepsilon_z[. \quad (61)$$

Proof . According to condition (23), we have

$$\rho^{(ii)}(0) = \rho^{(i)}(0) = \rho_0, \quad T^{(ii)}(0) = T^{(i)}(0) = T_0.$$

On the other hand, from the expressions for $D_1(\rho, T, c_0)$ and $D_2(\rho, T, c_0)$ given by (58) and (59), we can see that

$$D_1(\rho_0, T_0, c^{(i)}) > D_1(\rho_0, T_0, c^{(ii)}), \quad D_2(\rho_0, T_0, c^{(i)}) > D_2(\rho_0, T_0, c^{(ii)}),$$

291 which implies that (61) is satisfied in the neighborhood of $z = 0$. The lemma is proven. \square

292 Now, we will prove Lemma 4.

Proof of Lemma 4 The functions $\rho(z)$ and $T(z)$ that satisfy equations (20) and (48) are decreasing; this follows immediately from (56), (58) and (59). Suppose that relation (50) is not satisfied. This is equivalent to assuming that there exists a $z > 0$ such that

$$\rho^{(ii)}(z)T^{(ii)}(z) \geq \rho^{(i)}(z)T^{(i)}(z).$$

293 This hypothesis implies that there exists a $z_1 > 0$ such that

$$\rho^{(ii)}(z_1)T^{(ii)}(z_1) = \rho^{(i)}(z_1)T^{(i)}(z_1), \quad \rho^{(ii)}(z)T^{(ii)}(z) < \rho^{(i)}(z)T^{(i)}(z) \quad \forall z \in]0, z_1[, \quad (62)$$

$$\frac{d}{dz}(\rho^{(ii)}T^{(ii)})_{z=z_1} \geq \frac{d}{dz}(\rho^{(i)}T^{(i)})_{z=z_1}. \quad (63)$$

This implies that

$$\rho^{(ii)}(z_1) \leq \rho^{(i)}(z_1) - (c^{(ii)} - c^{(i)})$$

294 and according to (62) we conclude that

$$\rho^{(ii)}(z_1) < \rho^{(i)}(z_1), \quad T^{(ii)}(z_1) > T^{(i)}(z_1). \quad (64)$$

295 Relations (64) and (62), in addition to Lemma 6, imply that there exists a $z_0 \in]0, z_1[$
296 such that

$$\rho^{(ii)}(z_0) < \rho^{(i)}(z_0), \quad T^{(ii)}(z_0) = T^{(i)}(z_0), \quad T^{(ii)}(z) < T^{(i)}(z) \quad \forall z \in]0, z_0[. \quad (65)$$

297 The last two relations give

$$\frac{d}{dz}T^{(ii)}(z) \geq \frac{d}{dz}T^{(i)}(z) \quad \text{at } z = z_0. \quad (66)$$



298 By virtue of (57), the inequality $\rho^{(ii)}(z_0) < \rho^{(i)}(z_0)$ implies that inequality (66) cannot be
 299 satisfied. Therefore, our hypothesis of the existence of a $z > 0$ satisfying $\rho^{(ii)}(z)T^{(ii)}(z) \geq$
 300 $\rho^{(i)}(z)T^{(i)}(z)$ cannot be satisfied. Thus, inequality (50) is proven.

We have already proven that there is no $z_0 > 0$ for which

$$T^{(ii)}(z_0) = T^{(i)}(z_0), \quad T^{(ii)}(z) < T^{(i)}(z) \quad \forall z \in]0, z_0[, \quad \rho^{(ii)}(z_0) < \rho^{(i)}(z_0).$$

If

$$T^{(ii)}(z_0) = T^{(i)}(z_0), \quad T^{(ii)}(z) < T^{(i)}(z) \quad \forall z \in]0, z_0[, \quad \rho^{(ii)}(z_0) \geq \rho^{(i)}(z_0),$$

there would exist a $z' \in]0, z_0]$ such that

$$\rho^{(ii)}(z')T^{(ii)}(z') = \rho^{(i)}(z')T^{(i)}(z'),$$

301 which contradicts (50), thus establishing (49). Lemma 4 is proven. \square

302 7 NUMERICAL METHOD FOR THE STATIONARY SOLUTION

303 This section details the numerical methodology employed to determine the stationary solu-
 304 tion of the model, building upon the theoretical framework established in the preceding
 305 sections.

306 **Robustness and Efficiency** The numerical resolution of the parameter c_0 is performed
 307 using a numerical root-finding function, such as `fsolve` from Python's `scipy.optimize`
 308 library. As defined by the model's physics, \mathbf{c}_0 is directly related to the total stationary
 309 quantity of liquid/solid water Σ by the relation $\mathbf{c}_0 = \mathbf{g}\Sigma$. This function seeks the root
 310 of an objective function, i.e., the value of c_0 for which the pressure condition at the top
 311 ($\rho(\bar{z}_1)T(\bar{z}_1) - q_0 = 0$) is satisfied.

312 The root-finding algorithm efficiently converges to the required value of c_0 . For ex-
 313 ample, for the partially humid state, the algorithm identifies a value of c_0 that makes the
 314 objective function very close to zero, ensuring precise satisfaction of the physical condition
 315 at the top boundary.

316 **Interpretation of the Process:** The convergence process is robust and rapid. The
 317 algorithm progressively adjusts the value of c_0 until the objective function is minimized
 318 to a value very close to zero. This ensures that the final calculated profiles of density and
 319 temperature satisfy the top boundary pressure condition with high precision.

320 This process illustrates the robustness of the numerical method used to determine
 321 the parameters of the stationary solution, ensuring a precise convergence to the imposed
 322 physical conditions.



323 **Description of the solveStationary Implementation** The `solveStationary.py`
324 file implements the methodology for finding the stationary solution of the model, as
325 described in Proposition 5.1 of the article. The objective is to determine a set of sta-
326 tionary profiles for density $\rho(z)$, temperature $T(z)$, as well as constants α (intensity co-
327 efficient) and Σ (total quantity of liquid/solid water), satisfying the stationary equations
328 and boundary conditions.

329 The key steps of the process, as coded, are as follows:

330 **Initialization of constants and boundary conditions at $z = 0$** The code begins by
331 defining the physical constants (`g`, `R1`, `cv`, `z_bar_1`, `b_phi`) as well as the initial conditions
332 at the base of the "chimney" ($z = 0$): the initial density ρ_0 and the initial temperature
333 T_0 . These values serve as a starting point for the spatial integration towards $z = z_1$.

334 **Automated calculation of the top boundary condition (q_0)** A crucial aspect is the
335 automation of the q_0 calculation, defined as $q_0 = \rho(z_1)T(z_1)$ for the external hydrostatic
336 state. The code uses the `getHydrostaticProfiles.py` function, which models this state
337 with $\vartheta = 2/3$ (partially humid case), by receiving the same initial values (ρ_0, T_0) as input.
338 This automatically provides the target value q_0^{target} (external top pressure at $z_1 =$
339 10 000 m), to which the internal solution must be adjusted.

340 **Search for c_0 via a numerical root-finding function** The resolution relies on finding
341 the parameter c_0 (such that $c_0 = g\Sigma$) that satisfies the pressure condition at the top
342 boundary. This condition ensures that the calculated product $\rho(\bar{z}_1)T(\bar{z}_1)$ matches the
343 target value q_0 , where $R_1\rho(\bar{z}_1)T(\bar{z}_1)$ represents the pressure $P(\bar{z}_1)$ of the internal solution.
344 The stationary system (equations (20) and (48)) leads to the following formulation:

$$f(c_0) = \rho(\bar{z}_1)T(\bar{z}_1) - q_0 = 0.$$

345 A numerical root-finding function is used to solve this equation. It relies on an objective
346 function, `get_rhoT_at_z1.py`, which calculates $\rho(\bar{z}_1)T(\bar{z}_1)$ for each proposed c_0 value.
347 This process numerically implements the theoretical relation $c_0 = \nu^{-1}(q_0)$ by identifying
348 the c_0 value that makes $\nu(c_0)$ equal to the target q_0 .

349 **Resolution of solveSpatialProfilesHelper** The `solveSpatialProfiles_helper.py`
350 function performs an explicit numerical integration (Euler type) of the system equations
351 from $z = 0$ to $z = \bar{z}_1$, for a given c_0 value. At each spatial step, a 2×2 linear system is
352 solved (matrix M and vector V derived from equations (20) and (48)) to obtain $\frac{dT}{dz}$ and
353 $\frac{d\rho}{dz}$, and update the profiles.

354 This function also calculates the integral necessary for the evaluation of α , namely:

$$\int_0^{\bar{z}_1} \left(\bar{\pi}_{\text{vs}}(T) \frac{d}{dz} \log \rho - \frac{d}{dz} \bar{\pi}_{\text{vs}}(T) \right) dz.$$



355 Robustness tests are integrated to detect singular matrices, negative densities, or non-
 356 physical values (NaN, Inf), and to interrupt the procedure with a failure signal for the
 357 root-finding function.

358 **Calculation of stationary Σ and α** Once c_0 is determined by the root-finding func-
 359 tion, the stationary value of Σ is obtained by the defining relation $\mathbf{c}_0 = \mathbf{g}\Sigma$:

$$\Sigma^{\text{stat}} = \frac{c_0}{g}.$$

360 The value of α is then calculated from equation (55):

$$\alpha^{\text{stat}} = \frac{\Sigma^{\text{stat}}}{\frac{b}{\bar{z}_1} \int_0^{\bar{z}_1} \left(\bar{\pi}_{vs}(T) \frac{d}{dz} \log \rho - \frac{d}{dz} \bar{\pi}_{vs}(T) \right) dz}.$$

361 This final step uses the Σ^{stat} value derived from c_0 and the integral evaluated from the
 362 (ρ, T) profiles obtained with that c_0 .

363 **Advantages of the Approach** This method provides a stationary solution in a
 364 robust and automated manner. The use of a numerical root-finding function en-
 365 sures precise satisfaction of the pressure condition at the top. The automation of
 366 q_0 calculation, as well as the modularity of the functions (`getHydrostaticProfiles`,
 367 `solveSpatialProfiles_helper`), allows flexible exploration of different initial condi-
 368 tions, facilitating model validation.

369 8 NUMERICAL EXAMPLES

370 This section presents examples of numerical solutions obtained for the systems of equations
 371 studied in this article. We first illustrate the results for the stationary solution, whose
 372 existence and uniqueness have been established in the preceding sections. The numerical
 373 implementation of these models can benefit from specialized scientific computing software
 374 packages (Petrov et al., 2018). Then, we revisit the full evolutionary model to highlight
 375 the observed oscillatory behaviors, providing insight into the temporal dynamics of the
 376 system.

377 **Numerical Results for the Stationary Solution** We present examples of numer-
 378 ical solutions for the system (20)–(22), whose existence and uniqueness have been es-
 379 tablished. For the physical coefficients, we use: $g = 9.8 \text{ m/s}^2$, $R_0 = 8.314 \text{ J}/(\text{mol K})$,
 380 $\mu_a = 28.96 \text{ g/mol}$, and the temperature-dependent latent heat $L_{tr}(T) = (3244 - 2.72 T) \times$
 381 10^3 J/kg . We recall $R_1 = R_0/\mu_a$, $c_v = \frac{5}{2}R_1$, and the expression for $\bar{\pi}_{vs}(T)$ specified in
 382 (25). The value $\mathbf{c}_v = \frac{5}{2}\mathbf{R}_1$ is consistent with the standard value for a diatomic gas.

383 **Note on the Latent Heat L_{tr} :** The analytic proofs (notably Lemma 4.3 and the
 384 existence proof) treat the latent heat L_{tr} as a constant parameter for simplification,



385 which is sufficient to establish the necessary monotonicity and uniqueness. However,
 386 in the numerical implementation, we utilize the temperature-dependent expression
 387 $L_{tr}(T)$, as defined above, for enhanced physical realism and precision in the com-
 388 puted profiles. This approach ensures the robustness of the theoretical proof while
 389 maintaining the accuracy of the numerical results.

390 We set $\bar{z}_1 = 10\,000$ m, $\rho_0 = 1.2055$ kg/m³ and $T_0 = 293$ K. Two cases are ana-
 391 lyzed: a dry state ($\vartheta = 0$) with $q_0 = 85.51$ kg K/m³ and a moist state ($\vartheta = 2/3$)
 392 with $q_0 = 94.08$ kg K/m³. For these cases, the values of Σ obtained are respectively
 393 $\Sigma = 0.0562$ kg/m³ and $\Sigma = 0.0153$ kg/m³. Each q_0 value corresponds to the product
 394 $\rho(\bar{z}_1) \cdot T(\bar{z}_1)$ derived from the solution of the hydrostatic state problem (26)–(28). The
 395 distribution of $\rho(z)$ and $T(z)$ is consistent with natural observations. The temperature
 396 profile for the humid case deviates significantly from the dry case due to latent heat re-
 397 lease, while density profiles remain nearly identical as the atmosphere stays in hydrostatic
 398 equilibrium. Figure 2 illustrates the continuity and strict decrease of the function $\nu(\Sigma)$
 399 defined in (52), which is crucial for the existence proof.

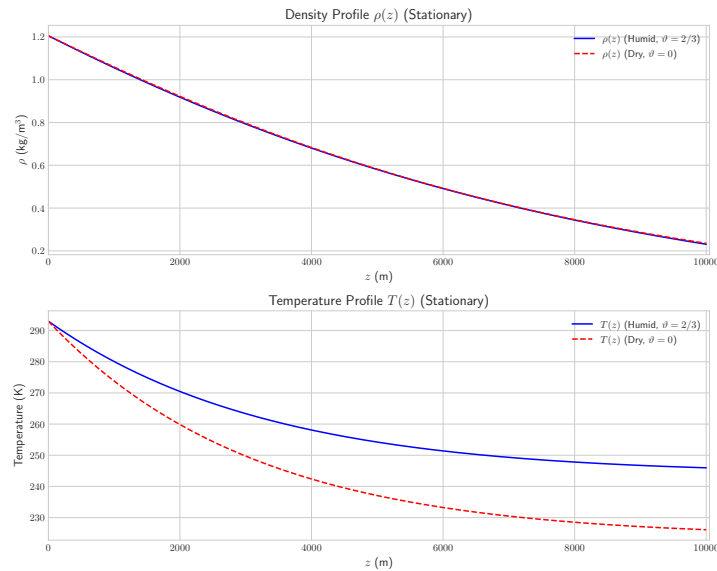


Figure 1: Distribution of density and temperature for the stationary solution (dry case, $\vartheta = 0$ and humid case, $\vartheta = 2/3$).

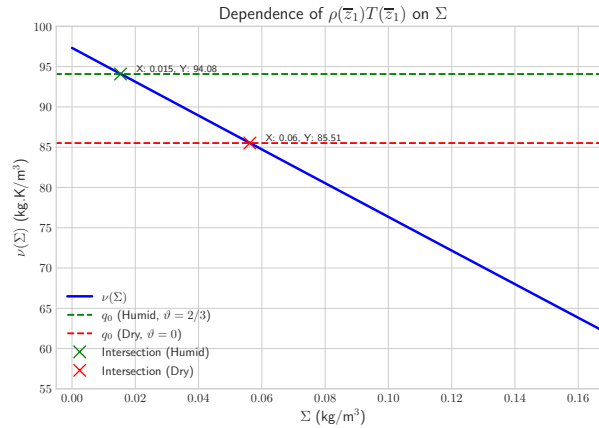


Figure 2: Dependence of $\rho(\bar{z}_1)T(\bar{z}_1)$ as a function of Σ .

400 **Numerical Results of the Evolutionary Model: Oscillations** As discussed in
 401 the motivation, the stationary solution's existence is vital when the evolutionary system
 402 (10)–(13) exhibits oscillations. Following the finite difference method detailed in (Bourega
 403 et al., 2018), we illustrate a damped oscillatory behavior using $b = 450$, $\vartheta = 2/3$, and
 404 discretization steps $h_t = 10$ s and $h_z = 10$ m. This value of b , representing the mean
 405 droplet residence time, ensures the numerical stability and the damping of the oscillations
 406 toward the stationary state.

407 Figure 3 presents the results for $\alpha(t)$ and $\Sigma(t)$ with $\rho_0 = 1.2055$ kg/m³, $T_0 = 293$ K, and
 408 $\bar{z}_1 = 10\,000$ m, showing damped oscillations over 7400 s. The strong correlation between
 409 $\alpha(t)$ and $\Sigma(t)$ suggests a cyclical mechanism: ascending humid air produces water, which
 410 accumulates and slows the ascent; the resulting decrease in water production then allows
 411 the air to resume a faster ascent.

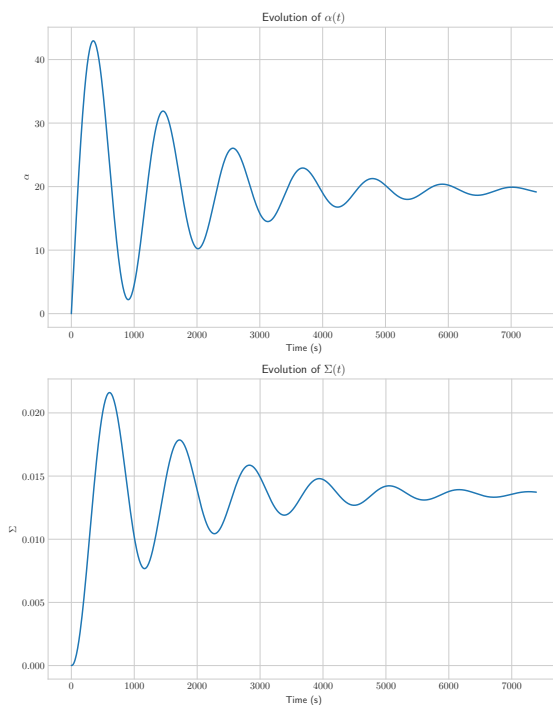
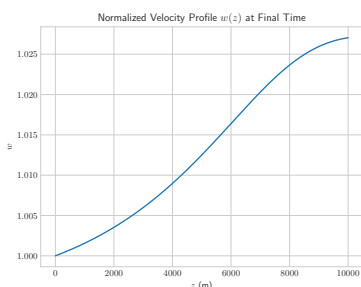


Figure 3: Damped oscillations of $\alpha(t)$ and $\Sigma(t)$.

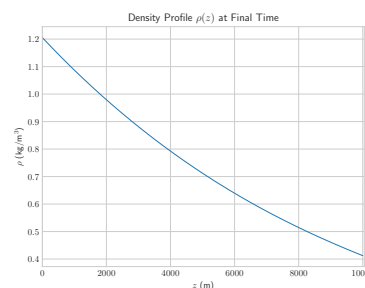
412 A significant finding is that $\Sigma(t)$ and $\alpha(t)$ stabilize at constant values remarkably
 413 consistent with the humid stationary solution ($\vartheta = 2/3$). This agreement provides a robust
 414 validation: the variables converge precisely toward $\Sigma_{\text{stat}} \approx 0.0153$ and $\alpha_{\text{stat}} \approx 32.87$ (Table
 415 1). Furthermore, the comparison highlights the role of latent heat: in the dry case, the
 416 coupling parameter α_{stat} must be significantly higher (≈ 120.03) to sustain the convective
 417 cell, whereas moist processes facilitate upward motion with a lower forcing threshold.

Table 1: Summary of Stationary Solution Parameters.

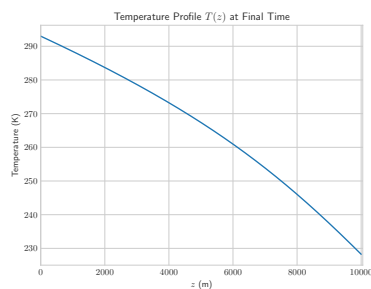
Case	c_0	$\Sigma_{\text{stat}} \text{ (kg/m}^3\text{)}$	α_{stat}
Humid ($\vartheta = 2/3$)	0.150241	0.015331	32.872555
Dry ($\vartheta = 0$)	0.550882	0.056212	120.034341



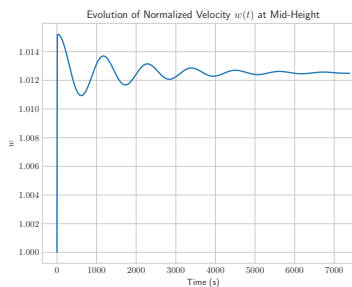
(a) Normalized velocity profile $w(z)$ at final time.



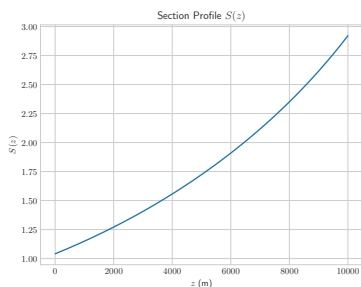
(b) Density profile $\rho(z)$ at final time of the evolutionary simulation. This shows the convergence of the evolutionary model to a stable density distribution, consistent with the humid stationary state.



(c) Temperature profile $T(z)$ at final time of the evolutionary simulation. This profile demonstrates the convergence of the evolutionary model towards a stable state.



(d) Evolution of normalized velocity $w(t)$ at mid-height.



(e) Section profile $S(z)$.

Figure 4: Results of the evolutionary simulation of the model. These figures complement the oscillation analysis presented in Figure 3.



9 OSCILLATORY DYNAMICS: THE VOLTERRA MODEL

418

419 As indicated in the introduction, the oscillatory behavior observed in our mathematical
 420 thunderstorm model, particularly for the variables $\alpha(t)$ and $\Sigma(t)$, exhibits striking analog-
 421 gies with the solutions of Volterra integro-differential equations. These equations are
 422 fundamental for describing dynamic systems that incorporate "memory" effects, where
 423 the future state depends not only on the current state but also on the entire past history
 424 of the system. The phenomenon of oscillation in these equations is a well-established
 425 area of mathematical literature, as noted by Volterra himself in his pioneering work on
 426 population dynamics (Volterra, 1931), and further developed by more recent studies such
 427 as those by Gopalsamy (Gopalsamy, 1987).

428 To explore this analogy, we consider the following Volterra integro-differential equa-
 429 tion, which is a specific form relevant to our comparison:

$$y'(t) = -a \int_0^t K(t-s)(y(s) - c)ds + d, \quad (67)$$

430 where $y(t)$ is the state variable, and $K(\tau) = \exp\left(-\frac{\pi\tau^2}{4b^2}\right)$ is the convolution kernel (a
 431 positive Gaussian function that decays rapidly, modeling the influence of past events).
 432 The parameters a , b , c , and d are positive constants. The equation is complemented by
 433 an initial condition $y(0) = \eta$.

434 To facilitate a qualitative comparison with the $\Sigma(t)$ variable of our thunderstorm
 435 model, which represents a physical quantity that must always be positive, we define a
 436 function $\Psi(t)$ as the integral of the product of the kernel $K(t-s)$ by the solution $y(s)$,
 437 modulated by the coefficient a :

$$\Psi(t) = a \int_0^t K(t-s)y(s)ds. \quad (68)$$

438 Since $a > 0$, $K(\tau) > 0$, and we expect $y(t)$ to remain positive (like $\alpha(t)$ in our model),
 439 this function $\Psi(t)$ is designed to always be positive, thus reflecting the behavior of $\Sigma(t)$.

440 Equation (67) can then be rewritten to highlight the relationship between $y'(t)$, $\Psi(t)$,
 441 and the other terms:

$$\begin{aligned} y'(t) &= -a \int_0^t K(t-s)y(s)ds + ac \int_0^t K(t-s)ds + d \\ y'(t) &= -\Psi(t) + \left(ac \int_0^t K(t-s)ds + d \right). \end{aligned}$$

442 The term in parentheses, $f(t) = ac \int_0^t K(t-s)ds + d$, acts as a forcing function.

443 **Challenges of Numerical Simulation** The numerical solution of integro-differential
 444 equations like (67) is not trivial. Unlike classical ordinary differential equations where
 445 the derivative depends only on the current state, here, the derivative $y'(t)$ depends on
 446 an integral that accumulates the influence of all past values of $y(s)$ up to time t . This



447 requires an iterative approach where, at each time step, the integral must be recalculated
448 by summing over all previous time points. We used a numerical method based on temporal
449 discretization (Euler’s method for the ODE) and a Riemann sum approximation for the
450 integral term, which demands careful management of temporal dependencies.

Simulation Results and Theoretical Justification For our simulation, we used parameters chosen to reinforce the analogy with our evolutionary storm model, specifically setting the memory parameter to $b = 450$. The values used are:

$$a = 3 \times 10^{-5}, \quad b = 450, \quad c = 1.2, \quad d = 1 \times 10^{-5}, \quad \eta = 0.01.$$

451 The simulation was conducted over a duration of 7200s to match the timescale of the
452 physical model. This choice of parameters allows for a precise physical analogy:

- 453 • Coupling (a): Represents the weight or negative buoyancy effect, dictating how
454 strongly the accumulated water Σ slows down the air intensity α .
- 455 • Memory (b): Represents the mean droplet residence time, governing the time delay
456 between condensation and the mechanical braking effect.
- 457 • Target (c): Corresponds to the stationary state α_{stat} toward which the system nat-
458 urally gravitates.
- 459 • Forcing (d): Represents the thermal instability (the energy engine) that drives the
460 convective motion.
- 461 • Initial Pulse (η): Reflects the initial updraft intensity $\alpha(0)$ required to trigger the
462 cycle.

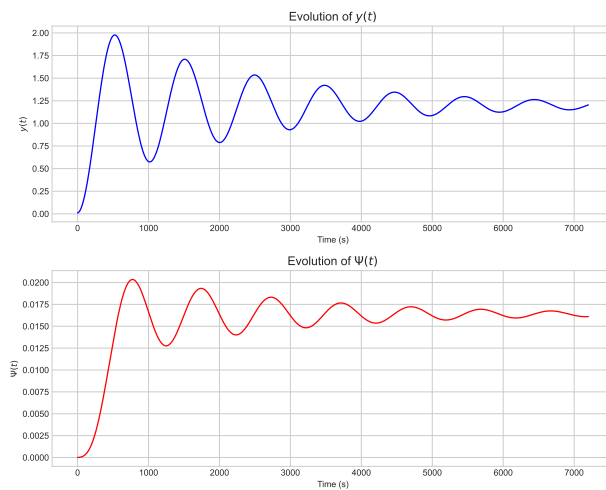


Figure 5: Damped oscillations of the Volterra equation solution. Upper panel: Evolution of $y(t)$. Lower panel: Evolution of $\Psi(t)$.



463 We clearly observe that $y(t)$ exhibits damped oscillations that converge towards an
464 equilibrium value, mirroring the behavior of $\alpha(t)$. The function $\Psi(t)$ remains always
465 positive and also displays damped oscillations, consistent with the physical nature of
466 $\Sigma(t)$. This dynamic correlation—where high $y(t)$ leads to an increase in $\Psi(t)$ —illustrates
467 the feedback mechanism where past states influence future dynamics via the Gaussian
468 kernel $K(\tau)$.

469 The works of Gopalsamy (Gopalsamy, 1987) and others provide conditions for the
470 existence of oscillations in integro-differential equations. While our specific formulation
471 (67) with positive parameters may not satisfy every strict constraint of existing theorems
472 (such as integrability over an infinite interval), the qualitative behavior observed is fully
473 consistent with the expected dynamics for systems with memory effects and restoring
474 forces.

475 In conclusion, this simulation of the Volterra equation serves as a powerful mathemat-
476 ical analogy for understanding the damped oscillations of our thunderstorm model. It
477 highlights that systems with memory and feedback mechanisms naturally generate such
478 dynamics. The synchronized qualitative analogy between (y, Ψ) and (α, Σ) , both gov-
479 erned by a similar residence time parameter $b = 450$, strengthens the understanding of
480 the complex physical phenomena at play.



481

10 CONCLUSION

482 The complete evolutionary system (10)–(14), previously studied in (Bourega et al., 2018),
483 describes complex atmospheric phenomena driven by ascending air flow and condensation.
484 This article has significantly advanced our understanding by focusing on the stationary
485 solution of a simplified version of this system.

486 The main contributions of this work are as follows:

- 487 1. We have successfully demonstrated the existence and uniqueness of the stationary
488 solution for the system (20)–(24) under the technical condition $T > \Theta_1$. This
489 theoretical result provides a rigorous mathematical basis for the long-term behavior
490 of such atmospheric models.
- 491 2. Numerical examples illustrate the validity of these results, showing that the moist
492 case ($\vartheta = 2/3$) yields higher temperatures than the dry case due to latent heat re-
493 lease, while maintaining consistent density distributions in hydrostatic equilibrium.
- 494 3. The analysis of the full evolutionary model revealed damped oscillatory behaviors
495 of the intensity coefficient $\alpha(t)$ and liquid water content $\Sigma(t)$. The fact that these
496 variables stabilize at the exact values predicted by the stationary solution provides
497 a robust validation of our analytical framework.
- 498 4. The qualitative analogy with the Volterra integro-differential equation, using the
499 consistent residence time parameter $b = 450$, highlighted striking mathematical
500 similarities. This suggests that the oscillations are a self-regulating cycle driven by
501 memory effects and restoring forces.

502 In conclusion, this study contributes to the mathematical modeling of atmospheric
503 processes by providing both a rigorous analytical framework for stationary states and
504 deeper insights into oscillatory dynamics. Future work could involve extending the exis-
505 tence and uniqueness proofs to more general conditions and exploring the implications of
506 these oscillatory behaviors for real-world weather events.

507

DATA AVAILABILITY

508 No external or experimental data sets were used in this theoretical study. The numerical
509 simulations presented in Sections 7, 8, and 9 were generated using custom Python scripts.
510 The code is available from the corresponding author upon reasonable request.

511

ACKNOWLEDGMENTS

512 The author would like to express her gratitude to Prof. Hisao Fujita Yashima (National
513 Higher School of Mathematics; NHSM-Sidi Abdellah, Algeria) for the useful discussions
514 and valuable insights that contributed to the realization of this article. The author also
515 thanks the Research Laboratory in Pure and Applied Mathematics (LRMPA) at USTO-
516 MB for the institutional support and providing the facilities to conduct this research.



517

FUNDING

518 The author received no financial support for the research, authorship, and/or publication
519 of this article.

520

COMPLIANCE WITH ETHICAL STANDARDS

521 This article does not contain any studies with human participants or animals performed
522 by the author.

523

AUTHOR CONTRIBUTIONS

524 D. R. Bourega designed the study, developed the mathematical proofs, performed the
525 numerical simulations, and wrote the manuscript.

526

COMPETING INTERESTS

527 The author declares that there are no competing interests.

528

References

529 Aouaouda, M., Ayadi, A., and Yashima, F. H.: Mathematical modeling of tropical cyclones
530 on the basis of wind trajectories, *Comput. Math. Math. Phys.*, 59, 1493–1507, 2019.

531 Bogovskii, M. E., Mantello, L., and Yashima-Fujita, H.: Solution to the stationary prob-
532 lem of glacier dynamics, *Comput. Math. Math. Phys.*, 50, 1734–1745, 2010.

533 Bourega, D. R., Aouaouda, M., and Fujita Yashima, H.: Rain oscillation in a mathemat-
534 ical model of a thunderstorm, *Ann. Math. Afr.*, 7, 19–35, 2018.

535 Cotton, W. R., Bryan, G. H., and Van den Heever, S. C.: *Storm and Cloud Dynamics*,
536 Elsevier, Amsterdam, 2nd edn., 2011.

537 Ghomrani, S., Marín Antuña, J., and Fujita Yashima, H.: A model of air ascent caused
538 by vapor condensation and its numerical calculation, *Rev. Cubana Fis.*, 32, 3–8, 2015.

539 Gopalsamy, S. K.: Oscillations in integrodifferential equations of arbitrary order, *J. Math.*
540 *Anal. Appl.*, 126, 100–109, 1987.

541 Hittmeir, S., Klein, R., Li, J., and Titi, E. S.: Global well-posedness for passively trans-
542 ported nonlinear moisture dynamics with phase changes, *Nonlinearity*, 30, 3676–3718,
543 2017.

544 Kikoine, A. K. and Kikoine, I. K.: *Molecular Physics*, Mir, Moscow, 1979.

545 Kouadri, S.: Qualitative behavior and stationary solutions for a class of atmospheric
546 models, *Results Appl. Math.*, 15, 100312, 2022.



- 547 Landau, L. D. and Lifshitz, E. M.: Fluid Mechanics, Mir, Moscow, 1989.
- 548 Mansour, M. A.: Stability analysis of non-linear dynamical systems in fluid flow applica-
549 tions, *Results Appl. Math.*, 12, 100 189, 2021.
- 550 Matveev, L. T.: Physics of the Atmosphere, Gidrometeoizdat, Leningrad-S. Peterburg,
551 2000.
- 552 Montgomery, M. T. and Smith, R. K.: Recent developments in the fluid dynamics of
553 tropical cyclones, *Annu. Rev. Fluid Mech.*, 49, 541–574, 2017.
- 554 Petrov, M. N., Tambova, A. A., Titarev, V. A., et al.: FlowModellium Software Package
555 for Calculating High-Speed Flows of Compressible Fluid, *Comput. Math. Math. Phys.*,
556 58, 1865–1886, 2018.
- 557 Plougonven, R. and Zhang, F.: Internal gravity waves from atmospheric jets and fronts,
558 *Rev. Geophys.*, 52, 33–76, 2014.
- 559 Prodi, F. and Battaglia, A.: *Meteorologia – Parte II, Microfisica*, Grafica Pucci, Roma,
560 2004.
- 561 Richiardone, R. and Manfrin, M.: A rain episode related to a mesoscale gravity wave,
562 *Bull. Am. Meteorol. Soc.*, 84, 1494–1498, 2003.
- 563 Volterra, V.: *Leçons sur la théorie mathématique de la lutte pour la vie*, Gauthier-Villars,
564 Paris, 1931.
- 565 Yashima, F. H.: Modeling the internal structure of tropical cyclones: flow equation on
566 wind trajectories, *J. Math. Sci.*, 242, 747–759, 2019.